

Warm rain processes over tropical oceans and climate implications

K. M. Lau¹ and H. T. Wu²

Received 5 September 2003; revised 17 November 2003; accepted 1 December 2003; published 30 December 2003.

[1] From analysis of TRMM data, we find that warm rain accounts for 31% of the total rain amount and 72% of the total rain area in the tropics, and plays an important role in regulating the moisture content of the tropical atmosphere. There is a substantial increase in precipitation efficiency of light warm rain as the sea surface temperature increases, but precipitation efficiency of heavy rain associated with deep convection is independent of sea surface temperature. This implies that in a warmer climate, there may be more warm rain, at the expense of less cloud water available for middle and high level clouds. *INDEX TERMS:* 1655 Global Change: Water cycles (1836); 1854 Hydrology: Precipitation (3354); 3360 Meteorology and Atmospheric Dynamics: Remote sensing; 3374 Meteorology and Atmospheric Dynamics: Tropical meteorology; 3314 Meteorology and Atmospheric Dynamics: Convective processes. **Citation:** Lau, K. M., and H. T. Wu, Warm rain processes over tropical oceans and climate implications, *Geophys. Res. Lett.*, 30(24), 2290, doi:10.1029/2003GL018567, 2003.

1. Introduction

[2] “Warm rain” refers to rain derived from non ice-phase processes in clouds. It is formed primarily by coalescence of water droplets of different sizes as they fall at different terminal velocities within the clouds. Warm rain processes are prevalent in marine clouds. However because sufficient liquid water and updraft are required to sustain collision-coalescence, warm rains are not restricted to low-to-middle level clouds, but may also occur in deep convective clouds [Glickman, 2000; Schumacher and Houze, 2003]. Warm rain is an integral component of the tropical precipitation system, contributing to heating and moistening of the lower troposphere, modifying stability, and possibly altering the recycling time scales of organized tropical convection [Johnson *et al.*, 1999; Johnson and Lin, 1997; Mapes, 2000; Wu, 2003; Del Genio and Kovan, 2002].

[3] Up to now, there have been no reliable estimates of the amount of warm rain and its role in the tropical water cycle. This paper attempts to provide a more quantitative description of warm rain processes taking advantage of the excellent data provided by the Tropical Rainfall Measuring Mission (TRMM). Launched in November 1997, TRMM has provided unique multi-year rain data that can be exploited for studies of the basic *modus operandi* of the tropical precipitation system. In this study, we use collocated TRMM products from December 1997 to August 2000 including rain rate of the TRMM Microwave Imager (TMI, 3G68), storm height (3A25) from the TRMM precipitation

radar, ratio of convective-to-total rain (2A23) [Kummerow *et al.*, 1998]. We also use total precipitable water, cloud liquid water content, and sea surface temperature derived from TMI by Wentz *et al.* [2000].

2. Identifying Warm Rain

[4] The retrieval of sea surface temperature (SST) from TMI using the low frequency (10.7 GHz) channel is contaminated in the presence of rain, because of the large blocking of the surface signal by the raindrops [Wentz *et al.*, 2000]. When a grid box ($0.25^\circ \times 0.25^\circ$ latitude-longitude) is completely covered with rain, no SST can be retrieved and the box is classified as undefined or NSST (no-SST). In the case of rain from broken clouds, or isolated showers that only partially cover a grid box, SST may still be derived from the neighboring non-rain pixels. As shown next, the distinction between rains in grid boxes with valid sea surface temperature (VSST) and NSST provides a viable separation between warm and cold rain processes.

[5] Figure 1 shows a snapshot of the spatial distribution of columnar cloud liquid water (CLW) of the VSST (upper panel) and NSST (lower panel) locations, averaged over a 3-day period January 1–3, 1998. The appearance of the cloud structure is typical of a period with active convection. At VSST locations, CLW is below 0.5 mm; the clouds consist of a mixture of tropical and subtropical systems including stratiform cloud filaments, remnants of anvil clouds, and isolated convective showers. Overall, the appearance of the cloud structure at VSST location suggests the presence of low-to-middle level clouds including *cumulus congestus*. The estimated percentage of convective-to-total rain in the VSST region is approximately 15%. On the other hand, as shown in Figure 1b, CLW at the NSST points generally exceeds 0.5 mm, and is largely confined to deep convection in the Intertropical Convergence Zone. The estimated percentage of convective rain in the NSST region exceeds 25%. The ratio of convective rain may be substantially underestimated both for NSST and VSST due to a possible error in the Version 5 2A23 algorithm, which classifies shallow, isolated warm rain showers as stratiform rain [Schumacher and Houze, 2003].

[6] Further delineation of the rain and cloud types associated with the VSST and NSST regimes can be seen from the storm height data. The storm height is defined as the highest altitude of threshold radar signal (= 18 dBz) from the TRMM precipitation radar [Short and Nakamura, 2000]. Storm heights below the freezing level at approximately 5 km can be identified with warm rains, and those above 5 km can be associated with cold rains. The distributions of storm heights (Figure 2a) show clearly that for NSST, the peak storm height is at approximately 6 km, above the freezing level. In contrast, the dominant storm heights for VSST are well below the freezing level at 2–

¹Laboratory for Atmospheres, NASA/Goddard Space Flight Center, Greenbelt, Maryland, USA.

²Science and Systems Application Inc., Lanham, Maryland, USA.

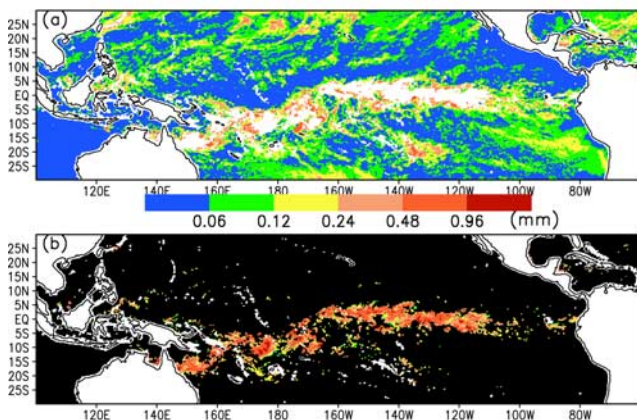


Figure 1. Spatial distribution of total column cloud liquid water at grid points with (a) valid SST (VSST), and (b) no-SST (NSST) for January 1–3, 1998.

3 km. Henceforth, we will identify the rain systems associated with VSST as warm rain, and NSST as cold rain. Note that considerable uncertainty exists in this definition of warm vs. cold rain, stemming from the ambiguity in distinguishing between liquid-phase and ice-phase rain at elevation higher than the freezing level. As shown later, for sustained rainrate >2 mm/hr, cold rain is high probable, and for rainrate <0.2 mm/hr, warm rain is quite certain. We estimate that 26% of VSST rain occurs at elevation above 5.5 km, of which 17% has a rainrate higher than 2 mm/hr. That means a possible upper bound in over-estimating warm rain by about 4% ($26\% \times 17\%$) in VSST rain, associated with the inability to separate supercooled water clouds above the freezing level from ice-phase rain. In NSST warm rain under deep convection will not be detected. We estimate that 32% of the NSST rain is derived from storm height lower than 4.5 km, of which about 31% has rainrate less than 0.2 mm/hr. This means that approximately 9–10% ($32\% \times 31\%$) of NSST rain may have been related to warm rain. Thus there is a possible cancellation of errors in the

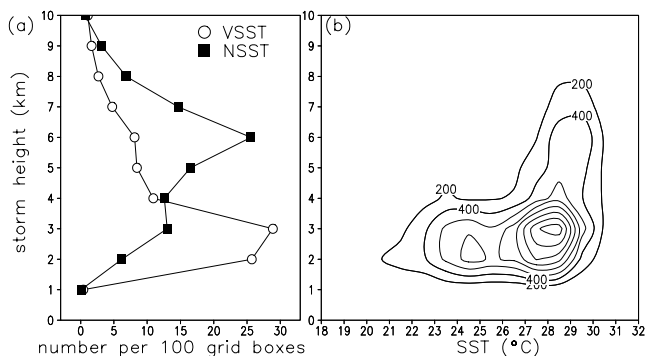


Figure 2. (a) Storm height distribution from tropical oceans (30°S to 30°N , 100°E to 60°W) of VSST and NSST points for January 1–3, 1998. (b) Joint probability distribution function of storm height and SST for the tropical oceans (30°S to 30°N , 100°E to 60°W) for January 1–3, 1998. Contour interval is 200. Unit is in number of occurrence within a bin of 1°C SST and 1 km storm height.

amount of warm rain vs. cold rain. However, because of the larger amount of warm rain possibly unaccounted for in NSST, we may have still underestimated the total warm rain in the tropics.

[7] For warm rain, Figure 2b shows the joint probability distribution function (PDF) of storm height and sea surface temperature across the entire Pacific Ocean basin. It is clear that the PDF is bimodal with warm rain having peak storm height at approximately 3 km over sea surface temperatures (SSTs) between $27\text{--}29^{\circ}\text{C}$, and a secondary storm height maximum of about 2 km for SSTs of $24\text{--}25^{\circ}\text{C}$. The former peak can be identified with low-to-middle level *cumulus congestus* in the warm pool region of the western Pacific. Some warm rains in this category are also associated with deep convection, as evident in the extended arm of the distribution with storm heights above 5 km. The secondary storm height maximum is related to stratiform rain, cloud debris or isolated showers.

3. Autoconversion Rate From Cloud-Rain Relationship

[8] Figure 3 shows a scatter plot of total surface rainrate vs. CLW for the period January 1–31, 1998. Similar features can be found for other periods and for different regions of the oceans. The warm-rain branch (open circles) shows largest concentration with low rainrate (<2 mm/hr) and small CLW (<0.5 mm). The warm rain shows a small population in the moderately convective (2–4 mm/hr) range, with relatively rare occurrence in the highly convective ($>4\text{--}6$ mm/hr) regime. For cold-rain (crosses), the population is skewed towards the intermediate-to-high convective regime, with rainrate >4 mm/hr, and CLW >0.8 mm. Heavy rainrates of over 8–10 mm/hr, and CLW over 1.4–1.6 mm are extremely rare for warm rains.

[9] To estimate the bulk autoconversion rate from the CLW-rainrate relationship, we use a parameterization scheme commonly used in the state-of-the-art weather and climate models with prognostic clouds [Sundqvist *et al.*, 1989; Tiedtke, 1993; Sud and Walker, 1999]. For a given cloud water content, the rate of release of precipitation P is

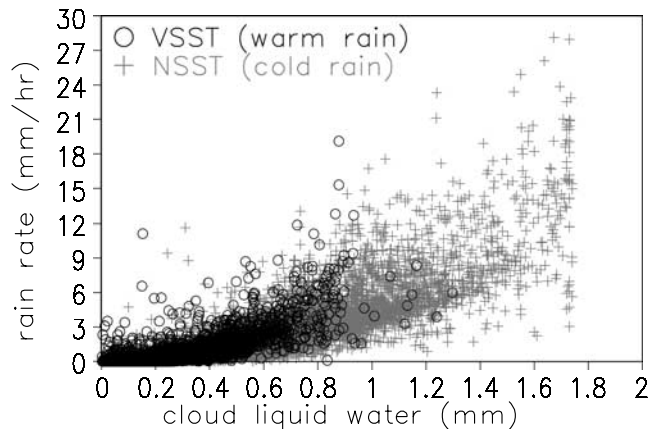


Figure 3. Scatter plot of collocated daily rainrate and CLW values from the eastern Pacific region (20°S – 20°N , 140°W – 85°W) for January 1–31, 1998.

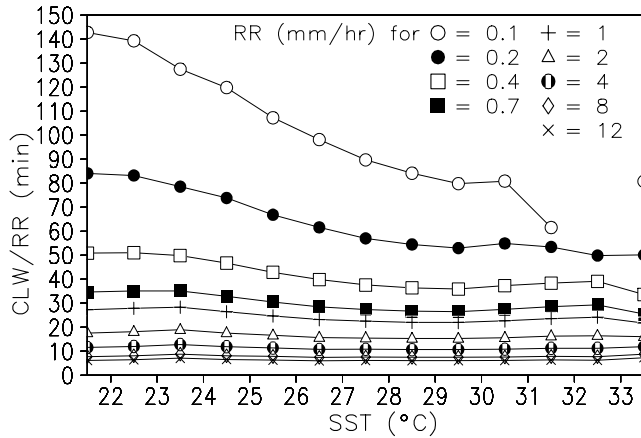


Figure 4. Residence time, defined as the ratio of cloud liquid water (CLW) to surface rainrate (RR) as a function of sea surface temperature (SST) and RR from collocated daily values from the eastern Pacific region (20° – 20° N 140° – 85°) for 12/8/1997–8/31/2000.

given by,

$$P = C_0 m \left[1 - \exp\left(-\frac{m^2}{m_r^2}\right) \right], \quad (1)$$

where m is the cloud water content, m_r a critical value of m ; C_0 indicates the efficiency of production of precipitation, with $1/C_0$ representing a characteristic time scale for conversion of cloud droplets to raindrops, i.e. the autoconversion time scale. The critical value m_r gives the typical value of cloud water content beyond which the collision-coalescence autoconversion of cloud drops to raindrops becomes substantial.

[10] The PDF of CLW-rainrate for the tropical Pacific and for the entire data period has been constructed for warm rain and cold rain respectively. Equation (1) with various parameters is superimposed on the PDF to obtain estimates of the bulk autoconversion time scale ($1/C_0$), and the critical CLW, m_r , that best fit the observational points. For warm rain, the estimated bulk autoconversion time scales are approximately 400–800 s, and a critical CLW of 0.6–0.8 mm, with a possible range of 200–1000 s, and 0.5–1.1 mm respectively. Similar range of time scales is also found for cold rain, where the critical CLW is approximately 0.9–1.1 mm, with a possible range of 0.8–1.2 mm. The larger critical CLW for cold-rain reflects the larger raindrop size for deep convection and ice-phase rain. Larger initial drop sizes are required to produce cold rain because the stronger updrafts advect cloud water to the supercooled zone and allow raindrops to grow larger before falling. The

TRMM derived autoconversion time scales are smaller by factors of 2–5 compared to those (1000–3000 s) used in the Sundqvist or similar parameterization schemes in climate models. The autoconversion rate may be an important source of model error, contributing to uncertainties in regional climate simulations and predictions [Sud and Walker, 1999; Sundqvist, 1989].

4. SST Dependence

[11] To illustrate the temperature dependence of the autoconversion process in warm rain, the daily rainrate and CLW data for the eastern Pacific region (20° S– 20° N, 140° W– 85° W) are binned according to SST. The binned data are then curve fitted to obtain the residence time, defined as the ratio of the CLW to rainrate. The following results are invariant for regions of similar size over the tropical oceans. From equation (1), for large CLW, the residence time approaches the bulk autoconversion time scale. For CLW much smaller than the critical value, the residence time varies as the inverse of the square of CLW, and can be much longer than the autoconversion time scale.

[12] Figure 4 shows the residence time as a function of SST for different rainrates. For light warm rains, defined here as the category of rain with rainrate less than 0.2 mm/hr, the residence time noticeably reduces (rainfall efficiency increases) as SST increases. For example, the residence time for the lowest rainrate (=0.1 mm/hr) category is about 2 hours at SST of 23–24°C and approximately one hour at 29–30°C. This implies an approximate doubling of the rainfall efficiency over a temperature increase of 6°C, or *an approximate 8–10% increase in rainfall efficiency per degree rise in SST*. The light warm rain is mostly associated with stratiform clouds, occupying more than 55% of the total area of warm rain, or over 17% of the total area of the tropics, but accounts for only about 4% of the total rain amount (see Table 1). Hence light warm rains may have large impact on the global radiation heat balance due to the associated large cloud coverage, even though it contributes only a small fraction of the total rain. As the rainrate increases, the residence time decreases, approaching a limit of 5–6 minutes for strongly convective rain. For heavy rain (>2 mm/hr), the autoconversion rate is largely independent of SST. This is likely due to the strong control of convective scale updraft on the autoconversion rates. As shown in Table 1, the fractional area of warm rain with rainrate greater than 2 mm/day is extremely small, less than 1.7% of the total rainy area, (= 0.5% of the total tropical area), but the contributed rain amount is more than 11% of total rain. This means that the heavy warm rain category, while insignificant in contributing to global radiation balance because of its small areal coverage, is important in contrib-

Table 1. Percentage Areal Coverage and Rainfall Amount for Warm (Cold) Rain Regimes for Light and Heavy Rain Category Respectively

Warm (cold) rain category	Percentage areal coverage of rainy area	Percentage areal coverage (all tropics, 30° S – 30° N)	Percentage of total rain amount
Light rain (<0.2 mm hr ⁻¹)	55 (7.8)	17.6 (2.5)	4.1 (8.8)
Heavy rain (>2 mm hr ⁻¹)	1.7 (5.6)	0.5 (1.8)	11 (47)
All categories	72 (28)	23 (9.0)	31.5 (68.5)

The second column is obtained by multiplying the first with the fraction rain (warm + cold) area to the entire tropics (=32%).

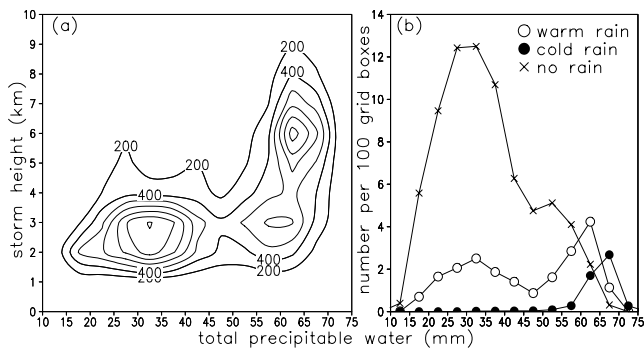


Figure 5. (a) Joint probability distribution function of storm height and total precipitable water from tropical oceans (30° to 30°N , 100° to 60°) for January 1–3, 1998. Contour interval is 200. Unit is in number of occurrence within a bin of 5 mm precipitable water and 1 km storm height. (b) Frequency distribution of total precipitable water for the same area and period as in (a) for warm rain, cold rain and no rain respectively. Units are normalized so that areas under the curve represent percentage of area of tropical oceans occupied by the rain category.

uting to the global water balance, and heat budget through the release of latent heat of condensation.

5. Moisture Regulation

[13] The importance of the warm rain in regulating the atmospheric moisture in the tropics is illustrated in Figure 5a where the joint PDF of total precipitable water (TPW) and storm height for the entire tropical ocean is shown. A trimodal distribution is discernable, with two maxima below, and one maximum above the freezing level. Comparing Figure 5a with Figure 2b, we infer that the first maximum (TPW = 30–35 mm, near 2–3 km) is associated with light warm rains ($R < 0.2$ mm/hr) from shallow clouds or isolated showers, over regions with cold SST ($< 26^{\circ}$). The second maximum of TPW ~ 60 mm near 3 km is largely associated with middle level clouds, including *cumulus congestus* over the warm pool (SST $> 28^{\circ}\text{C}$). The maximum TPW ~ 60 –65 mm near 6 km is associated with cold rains in the core of deep convection over the warm pool region.

[14] Figure 5b shows the frequency distributions of TPW of warm, and cold rains normalized by the total rain area. Also shown is the TPW distribution for the no-rain regions. The distributions confirm that the two TPW maxima below the freezing level are associated with warm rains, and that the TPW maximum (~ 65 –70 mm) above freezing level arises from cold rain processes. As noted from the areas under the curves, the areal coverage of warm rain is much larger than that of the cold rain. Specifically, Table 1 shows that warm rain covers 72% of the total rain area, or 23% of all tropical area, while accounting for approximately 31% of the total rain amount. The fractional amount of warm rain is higher than the 20% of rain from shallow clouds estimated by *Short and Nakamura* [2000]. This is because our definition of warm rain includes also related convective processes at elevations above the freezing level. Our warm rain amount compares favorably with the 28% estimated by *Johnson et al.* [1999] based on ground-based radar observations of cloud populations over the western Pacific warm

pool. The TPW distribution for the no-rain regions shows a pronounced maximum at ~ 25 –35 mm, coinciding with the lower maximum identified with light warm rains with storm height at 2–3 km (see also Figures 2b and 5a). This suggests that re-evaporation from falling warm rain may be important in contributing to, and in homogenizing the moisture content of the nearby no-rain regions. Interestingly, a moist zone with TPW ~ 45 –55 mm is found in the no-rain region. This moist zone is likely due to moistening from detrainment of warm rain from nearby middle level *cumulus congestus*. Since warm rains form over much larger area (23% tropical area) than cold rain (9%), and in the neighborhoods of convective as well as dry regions (68% tropical coverage), they may be important in regulating the moisture content of the *more than 90%* of the tropical area.

6. Climate Implications

[15] Based on the result that precipitation production per unit CLW for light warm rain increases as SST rises, it may be argued that in a warmer climate, more warm rain will be squeezed out from middle and low-level clouds. Precipitation laden air parcels associated with warm rain are less buoyant compared to the ambient air, hence less likely to organize into deep convection [*Johnson et al.*, 1999; *Rosenfeld and Lensky*, 1998]. As a result, an abundance of warm rain will desiccate the upper troposphere, and hence reduce upper level cloudiness and cold rain production. Such a scenario is consistent with the recent observation of a drying trend in the subtropics and reduction in tropical cloudiness [*Schroeder and McGuirk*, 1998; *Bates and Jackson*, 2001]. However, more warm rain may enhance low-level heating and moisture convergence [*Mapes*, 2000; *Wu*, 2003], leading to enhanced vertical moisture transport and increased upper level clouds and cold rain. More work is needed to unravel the effects of global warming on tropical convection and the global water cycle. Better understanding of warm rain processes and improved representation in climate models may hold the key to the success of such work.

[16] **Acknowledgments.** This work is supported by the Tropical Rainfall Measuring Mission (TRMM) Project of the NASA Earth Science Enterprise.

References

- Bates, J. J., and D. L. Jackson, Trends in upper tropospheric humidity, *Geophys. Res. Lett.*, 28, 1695–1698, 2001.
- Del Genio, A. D., and W. Kovan, Climatic properties of tropical precipitating convection under varying environmental conditions, *J. Clim.*, 15, 2597–2615, 2002.
- Glickman, T. S., (Ed.), *Glossary of Meteorology*, *Am. Meteorol. Soc.*, 855 pp, 2000.
- Johnson, R. H., and X. Lin, Episodic trade wind regimes over the western Pacific warm pool, *J. Atmos. Sci.*, 54, 2020–2034, 1997.
- Johnson, R. H., T. M. Rickenbach, S. A. Rutledge, P. E. Ciesielski, and W. H. Schubert, Trimodal characteristics of tropical convection, *J. Clim.*, 12, 2397–2418, 1999.
- Kummerow, C., W. Barnes, W. T. Kozu, J. Shiue, and J. Simpson, The Tropical Rainfall Measuring Mission (TRMM) Sensor Package, *J. Atmos. Oceanic Tech.*, 15, 808–816, 1998.
- Mapes, B. E., Convective inhibition, subgrid scale triggering energy, and stratiform instability in a toy tropical wave model, *J. Atmos. Sci.*, 57, 1515–1535, 2000.
- Rosenfeld, D., and I. M. Lensky, Space-borne sensed insights into precipitation formation processes in continental and marine clouds, *Bull. Am. Meteorol. Soc.*, 79, 2457–2476, 1998.

- Schroeder, S. R., and J. M. McGuirk, Widespread tropical atmospheric drying from 1979 to 1995, *Geophys. Res. Lett.*, 25, 1301–1304, 1998.
- Schumacher, C., and R. A. Houze, The TRMM precipitation radar view of shallow, isolated rain, *J. Appl. Meteorol.*, 42, 1519–1524, 2003.
- Short, D. A., and K. Nakamura, TRMM radar observations of shallow precipitation over the tropical oceans, *J. Clim.*, 13, 4107–4124, 2000.
- Sud, Y., and G. K. Walker, Microphysics of clouds with the relaxed Arakawa-Schubert cumulus scheme (McRAS), Part II: Implementation and performance in GEOS II GCM, *J. Atmos. Sci.*, 56, 3221–3240, 1999.
- Sundqvist, H., E. Berge, and J. E. Kristjansson, Condensation and cloud parameterization studies with a mesoscale numerical weather prediction model, *Mon. Wea. Rev.*, 117, 1641–1657, 1989.
- Tiedtke, M., Representation of clouds in large scale models, *Mon. Wea. Rev.*, 121, 3040–3061, 1993.
- Wentz, F. J., C. Gentemann, D. Smith, and D. Chelton, Satellite measurements of sea surface temperature through clouds, *Science*, 288, 847–850, 2000.
- Wu, Z., A shallow CISK, deep equilibrium mechanism for the interaction between large-scale convection and circulation in the tropics, *J. Atmos. Sci.*, 60, 377–392, 2003.
-
- K. M. Lau, Laboratory for Atmospheres, NASA/Goddard Space Flight Center, Greenbelt, MD, USA. (william.k.lau@nasa.gov)
- H. T. Wu, Science and Systems Application Inc., Lanham, MD, USA.